J. Biomedical Science and Engineering, 2015, 8, 257-273
Published Online April 2015 in SciRes. http://www.scirp.org/journal/jbise
http://dx.doi.org/10.4236/jbise.2015.84025

Rab1-Dependent Gβ1γ2 Trafficking during Muscle Mobilization

Hanwei Huang[1], Ting Li[1], Lei Geng[1], Hui Zhao[2*]

[1]Department of Integrative Medicine and Neurobiology, National Key Laboratory of Medical Neurobiology, Institute of Brain Sciences, Fudan University, Shanghai, China
[2]Department of Orthopaedics, Shanghai 5th Hospital, Fudan University, Shanghai, China
Email: *zhaohui07054@fudan.edu.cn

Received 8 January 2015; accepted 5 April 2015; published 14 April 2015

Abstract

Fyn kinase-dependent cellular events were related with skeletal muscle denervation. In the present study, we used a combination of techniques to measure ER stability and the related Gβ1γ2 trafficking following muscle mobilization, and demonstrated a temporally and Fyn-dependent up-regulation of Ca^{2+} level in the mobilized muscle. In parallel, Fyn activity in ER was gradually decreased, which was accompanied by enhanced PTP1B activity and expressions of ER proteins (calnexin, Grp94, cyclophilin, and Hsp70). Moreover, during muscle mobilization, there was more membrane protein breakdown than protein synthesis, which probably featured robust Gβ1γ2 internalization, and Rab1-dependent transport into ER compartment; the signaling was related to disruption of PI3K-Akt signaling and decrement of muscular functions. Then, Gβ1γ2 trafficking is a key component necessary for the early recovery processes regarding muscle atrophy, which would be the therapeutic consideration for muscle repair and regeneration.

Keywords

Muscle Mobilization, Fyn, Rab1, Gβ1γ2, Endoplasmic Reticulum

1. Introduction

Skeletal muscle comprises up to 40% of human body mass, which is a highly ordered, structurally stable tissue. Muscular function is dependent on intact nerve supply; for example, sciatic nerve injury causes profound structural and functional changes including rapid loss of muscle mass and contractile force [1] [2]. As reported, growth factors usually result in a quick and adaptive response, and mediate changes allowing an animal to effec-

*Corresponding author.

How to cite this paper: Huang, H.W., Li, T., Geng, L. and Zhao, H. (2015) Rab1-Dependent Gβ1γ2 Trafficking during Muscle Mobilization. *J. Biomedical Science and Engineering*, **8**, 257-273. http://dx.doi.org/10.4236/jbise.2015.84025

tively face mobilization [3]-[7]. Coincidently, we have characterized that Fyn, one of Src kinases, represented the predominant signaling in VEGFR-2 activation and VEGFR-1 shuttling between membrane and ER, which initiated stereotypic inflammation and muscle-T cell interaction during muscle denervation [8]-[10]. Therefore, it was proposed that subcellular communication might form a viable link to functional muscular stabilization.

As reported, Fyn-related signaling served as integral components for remodeling of G-protein-coupled receptors (GPCR) [11] [12]. As reported, heterotrimeric G protein signaling to the plasma membrane could be activated by GPCR, which promoted the exchange of GDP (guanosine diphosphate) for GTP in the Gα subunit and its dissociation from G$\beta\gamma$. GTP-loaded G$\beta\gamma$ served as part of the mechanism of PI3-kinase activation [13]-[16]; such examples included internalization of G$\beta\gamma$ in response to the action of β-adrenergic receptors. Additionally, this pool of free G$\beta\gamma$ is associated with endosomes, and capable to cause remodeling of Golgi apparatus [17]-[25].

Intracellular trafficking of diverse signal transduction proteins is coordinated by a variety of Rab GTPases that regulate the budding and fission of vesicles from compartments [23]-[25]; among them, Rab1 is a molecule for transport from ER to Golgi [14]-[16]. Then, it raised possibility that cross-link of G$\beta\gamma$-Rab1 might involve in muscle adaptation during muscle mobilization. A deeper understanding of phenotype-dependent stability of ER compartment would certainly provide insight into novel preventive or therapeutic regimens to alleviate or delay muscular damage.

2. Methods

2.1. Leg Casting Disuse Atrophy Model and Ethics Statement

Mice were anesthetized with isoflurane, and the lower right leg was casted from the knee to the toes with heat-activated casting material (Vet Lite, Kruuse, Marslev, Denmark). The test materials were administered by continuous infusion via implantation of an osmotic minipump. After casting, animals were euthanized by carbon dioxide asphyxiation followed by cervical dislocation. Gastrocnemius was dissected rapidly from both legs when the cast was removed, and the muscles were cleaned of tendons and connective tissue and weighed.

All experiments using animals were conducted in accordance with the relevant codes of practice for the care and use of animals for scientific purposes (National Institutes of Health, 1985). All experimental protocols were approved by Ethics Committee of Fudan University, all efforts were made to minimize the numbers of animal used and their suffering.

2.2. Immunohistochemistry

Serial sections of gastrocnemius were carried out on a cryostat at 15 μm. Sections were mounted on glass slides (Superfrost plus) and labeled with antibody against G$\beta1\gamma2$ (1:1000, Abcam, Cambridge, MA) and Alexa Fluor594 conjugated secondary antibody. Antibodies were diluted in 0.01M PB with 3% normal goat serum, 1% BSA, 0.5% Triton X-100, and 0.05% sodium azide, pH7.4. Sections were viewed under microscope (Leica L2000A), images were acquired and processed by Leica Quin software. In separate experiments, we tested different antigen retrieval techniques including microwave heating and SDS-pretreatment.

2.3. Satellite Cell Culture

Gastrocnemius was weighted after being cleaned of tendons and fat tissue, cut in fragments, rinsed in PBS, incubated in 15 ml of dissociation medium and incubated at 37˚C in a water bath for 1 h. Every 10 min tube was shaken gently. Afterwards, muscle fragments were dispersed using a 10 ml pipette with a large extremity in the presence of the dissociation medium. Supernatant was decanted and filtered through a 200 μm nylon mesh into a tube containing an equal volume of culture medium to isolate free cells. The remaining muscle tissue was further dissociated in fresh dissociation medium before being filtered in a tube to isolate additional free cells. Free cells were centrifuged (300 g, 10 min) and resuspended in 5 ml of DMEM with 10% (v/v) fetal bovine serum, then were seeded at a density of 6 - 10 × 10^4 cells per 25 cm^2 flask (Nunc) in a total volume of 4 ml culture medium. The cultures were grown at 37˚C with humidified atmosphere containing 5% CO_2. 4 days later, cells were assayed.

For macrophage or T cell induction, lipopolysaccharide (LPS, 100 ng/mL) and lymphocytes (1 × 10^6) were added to cultures for 48 hours. Conditioned medium was collected and concentrated 100-fold using Amicon ul-

tra centrifuge filters (Millipore, Billerica, MA, USA).

2.4. Assays for Protein Metabolism

Gastrocnemius was rinsed and homogenized, the precipitated proteins were collected by centrifugation. The supernatant was used for measurement of L-[3,4,5-^{3}H] phenylalanine specific activities. The pellet was washed three times in 2% (v/v) perchloric acid and then hydrolyzed in 2 M NaOH. The fractional protein synthesis rates were calculated using the equation: fr PS (% day) = Sb/Si·t, where Sb and Si are the specific activities of the protein-bound and free acid-soluble tissue phenylalanine pools respectively; t is the time after the isotope injection in days.

To assess protein breakdown rates, gastrocnemius was tied by the tendons at resting length to stainless steel supports and preincubated in a shaking water bath for 30 min at 37˚C in individual stoppered 25 ml flasks containing 3 ml oxygenated (95% O_2 - 5% CO_2) Krebs-Henseleit bicarbonate buffer (pH 7.4) with 10 mM glucose. Muscles were then incubated in fresh buffer containing 0.5 mM cycloheximide for 2 h. The net production of tyrosine and 1-methyl-histidine (1-Me-His) during incubation was assayed using HPLC. Incubation studies were carried out using 6 - 8 muscles per group, each gastrocnemius obtained from a separate rat.

2.5. Intracellular Ca^{2+} Measurement

One day before the assay, CORNING® black with clear flat bottom 96-well-assay plate was coated with poly-L-Lysine. Gastrocnemius was homogenized, suspended and plated in 150 µl medium and incubated in a humidified atmosphere of 5% CO_2 at 37˚C overnight. At the day of assay, 100 µl medium was removed from plate, 50 µl FLIPR® calcium assay reagent (Molecular Devices Corp) dissolved in 1× reagent buffer (1× HANKs buffer with 20 mM HEPES), pH 7.4, with 5 mM probenecid was added and the plate was incubated at 37˚C for 1 h. Treatment reagents were dissolved in the assay buffer (HBSS: KCl 5 mM, KH_2PO_4 0.3 mM, NaCl 138 mM, $NaHCO_3$ 4 mM, Na_2HPO_4 0.3 mM, D-glucose 5.6 mM, with additional 20 mM HEPES, 2.5 mM probenecid and 13 mM $CaCl_2$). Using a FlexStation (Molecular Devices Corp.), the $[Ca^{2+}]$i fluorescence were monitored every 1.52 s intervals with excitation wavelength at 485 nm and emission wavelength at 525 nm. The $[Ca^{2+}]$i fluorescence was measured up to 90 s, the fluorescence intensity from 3 wells were averaged and the relative amount of $[Ca^{2+}]$i release was determined by integrating the area under the peak of the $[Ca^{2+}]$i fluorescence averages.

2.6. Recombinant Adenovirus Construction

Recombinant adenovirus expressing mouse Gβ1γ2, Rab1 siRNA were constructed by inserting into the adenoviral shuttle vector pDE1sp1A (Microbix Biosystems, Inc., Canada), and the insert was then switched to the adenoviral vector through LR recombination. After homologous recombination with the backbone vector PJM17, plaques resulting from viral cytopathic effects were selected and expanded in 293 cells. Positive plaques were further purified and large-scale production of adenovirus was carried out by two sequential CsCl gradients and PD-10 Sephadex chromatography.

2.7. Subcellular Fractionation

For nuclear extracts, gastrocnemius was washed twice in ice-cold PBS, resuspended in buffer A (10 mM HEPES, 10 mM NaCl, 3 mM $MgCl_2$, 1 mM EGTA, 0.1% Triton X-100, pH 7.5) supplemented with 50 mM NaF, 1 mM Na_3VO_4, 1 mM DTT, 1 mM PMSF, and 1 µg/ml protease inhibitor cocktail and incubated on ice for 40 min. The nuclei were pelleted by centrifugation at 2400 g for 10 min at 4˚C and resuspended in buffer B (25 mM HEPES, 300 mM NaCl, 5 mM $MgCl_2$, 1 mM EGTA, 20% glycerol, pH 7.4) supplemented with 50 mM NaF, 1 mM Na_3VO_4, 1 mM DTT, 1 mM PMSF, and 1 µg/ml protease inhibitor cocktail. After incubation on ice for 60 min, the lysates were centrifuged at 12,000 g for 20 min at 4˚C. The supernatants (nuclear extracts) were collected and assayed.

For ER separation, gastrocnemius was homogenized in 2 ml of 10 mM Tris-HCl (pH 7.5) and 150 mM sucrose, the resulting cell lysate was mixed with 6.5 ml of 1 mM Tris-HCl (pH 7.5), 1 mM EDTA, and 63.5% sucrose and layered under a sucrose density gradient (1.5/1.7/2.1 M sucrose). Gradients were centrifuged at 100,000 ×g for 3 h and ER fractions were collected manually. ER fractions were washed with 2 vol. of 10 mM Tris-HCl (pH 7.5) with centrifugation, and resuspended in 10 mM Tris-HCl (pH 7.5) with 150 mM sucrose, then

stored for later analysis.

2.8. Immunoprecipitation and Western Blotting

Gastrocnemius was homogenized and centrifuged, the supernatants were incubated with anti-Rab1, AchRα antibody (1:200; BD Transduction Laboratories, Lexington, KY) at 4˚C overnight with slow rotation. 60 µl of protein G-agarose beads (Invitrogen, Carlsbad, CA) were added and further incubated for 3 h. Afterwards, the beads were washed and protein sample were eluted from with 1x SDS sample buffer.

For Western blot analysis, protein samples were resolved by sodium dodecylsulfate polyacrylamide gel electrophoresis (SDS-PAGE) and transferred to polyvinylidene difluoride membranes (GE Healthcare, Piscataway, NJ). Membranes were probed with anti-cSrc, anti-Gβ1γ2 (1:1000; Abcam, Cambridge, MA), anti-AchRβ (1:500; Abcam), anti-calnexin, anti-Grp94, anti-cyclophilin, anti-Hsp70 (1:500; BD Transduction Laboratories) respectively. Protein bands were detected using alkaline phosphatase conjugated secondary antibodies (1:5000) and ECF substrate, and then scanned using a Storm 860 imaging system. Band intensities were quantified and analyzed with ImageQuant software (GE Healthcare).

2.9. *In Vitro* Fyn and MuSK Kinase Assay

Proteins in anti-Fyn or anti-MuSK antibody immunoprecipitated pool (1:200; Abcam) were precipitated with 5% (w/v) TCA. The resulting pellets were washed with acetone and incubated at 30˚C with 5 µg of SRC substrate peptide (KVEKIGEGTYGVVYK, corresponding to amino acids 6 - 20 of p34cdc2; Upstate Biotechnology, Lake Placid, New York) in kinase buffer containing 5 µCi of [γ-^{32}P]-adenosine triphosphate ([γ-^{32}P]-ATP; PerkinElmer Life Sciences, Waltham, Massachusetts), 50 mM Tris-HCl (pH 7.5), 10 mM $MgCl_2$, 10 mM $MnCl_2$, 25 µM ATPase, 1 mM dithiothreitol, and 100 µM Na_3VO_4. After 30 min, the reaction was terminated by the addition of 10 µl of 40% (w/v) TCA, and samples were spotted on P81 cellulose phosphate paper (Upstate Biotech). The paper was washed three times with 1% (w/v) phosphoric acid and once with acetone. Radioactivity retained on the P81 paper was quantified by liquid scintillation counting. Blank counts (without tissue lysate) were subtracted from each result, and radioactivity (cpm) was converted to picomoles per minute (pmol/min).

2.10. PTP 1B Assay

Gastrocnemius was collected and homogenized in RIPA buffer (50 mM Tris [pH 7.5], 150 mM NaCl, 2 mM EDTA, 1.0% Triton X-100 and complete protease inhibitor mixture). Equal amounts of protein were incubated at 4˚C for 2 h with anti-PTP1B antibody and then, 20 µl of protein G sepharose was added and incubated for additional 2 h with mixing. Immunoprecipitated complexes were washed twice in RIPA buffer, once with the assay buffer (25 mM imidazole [pH 7.2], 0.1 mg/ml BSA, 10 mM DTT) and finally they were resuspended in 25 µl of assay buffer. The phosphatase substrate raytide was labeled at its unique tyrosine residue in the presence of [γ-^{32}P] ATP. Assay mixtures (30 µl) containing the immunoprecipitated pellet and [γ-^{32}P]-labeled raytide (1×10^5 cpm) were incubated at 30˚C for 2 h and the reaction was terminated by adding 750 µl of a charcoal mixture (0.9 M HCl, 90 mM sodium pyrophosphate, 2 mM NaH_2PO_4, 4% vol/vol Norit A). After centrifugation, the radioactivity in 400 µl of the supernatant was measured by scintillation counting. Blanks were determined by measuring the free γ-^{32}P in reactions where the immunoprecipitates were either boiled or omitted, and these values were subtracted from the reaction values.

2.11. Whole Muscle Mechanical Properties

The experiments were performed *in vitro* at 30˚C in a vertical muscle apparatus (300B, Aurora Scientific) containing a Ringer solution (120 mM NaCl, 4.7 mM KCl, 2.5 mM $CaCl_2$, 3.15 mM $MgCl_2$, 1.3 mM NaH_2PO_4, 25 mM $NaHCO_3$, 11 mM glucose, 30 µM d-tubocurarine, pH 7.2 - 7.4) continuously bubbled with 95%O_2 - 5%CO_2. The muscles were stretched to the optimal length, *i.e.*, the length that allowed maximal tension development in response to a single pulse. The muscles were then electrically stimulated, through two parallel electrodes, with supramaximal pulses (0.5 ms duration) delivered by a Grass S44 electronic stimulator through a stimulus isolation unit (Grass SIU5). Muscle response was recorded by isometric force transducer (Grass FT03). Data were analyzed by LabView software. Tetanic stimulation was obtained by applying trains of supramaximal stimuli at 80- and 150-Hz frequency for the muscles. Tetanic tension was normalized to the muscle wet weight (specific

tension, N/g). Muscles were weighed at the end of each experiment.

2.12. Statistics

Data were represented as mean ± SEM and analyzed with Prism 5 software. For all data sets, normality and homocedasticity assumptions were reached, validating the application of the one-way ANOVA, followed by Dunnett test as post hoc test to do comparisons. Differences were considered significant for $p < 0.05$.

3. Results

3.1. Temporal Alteration of ER in Response to Muscle Mobilization

In the present study, muscle mobilization was established by leg casting, 1, 7, 14 and 21 days later, extracellular Ca^{2+} levels in gastrocnemius were measured using FlexStation. As shown in **Figure 1(a)**, Ca^{2+} levels rose rapidly at day 1 - 7, which were approximately 2.4 and 2.1 folds over control in $Fyn^{(+/-)}$ mice, and 1.3 folds over control in $Fyn^{(-/-)}$ mice. Intriguingly, the elevation could be partly inhibited by thapsigargin (1 μM, 16 h), indicating that there might have functional alteration of ER during muscle mobilization. As a confirmation, it was demonstrated that following leg casting, Fyn activity was increased with compartment dependent manner, in ER, the elevation of [γ-^{32}P] incorporation was transient, which rose approximately 3.4 folds over control values within 7 days, instead in nucleus, Fyn activation happened persistently, which increased around 3.3 folds over control (**Figure 1(b)**). PTP1B activity was also investigated by [γ-^{32}P] incorporation, as demonstrated, PTP1B

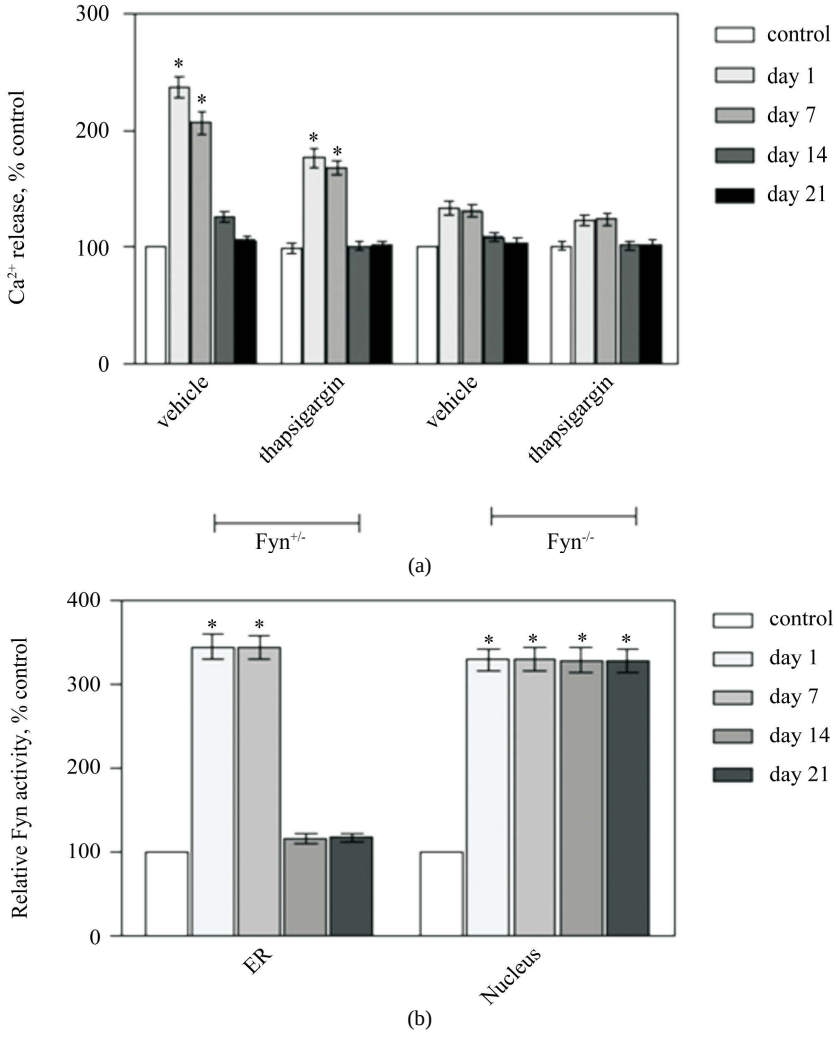

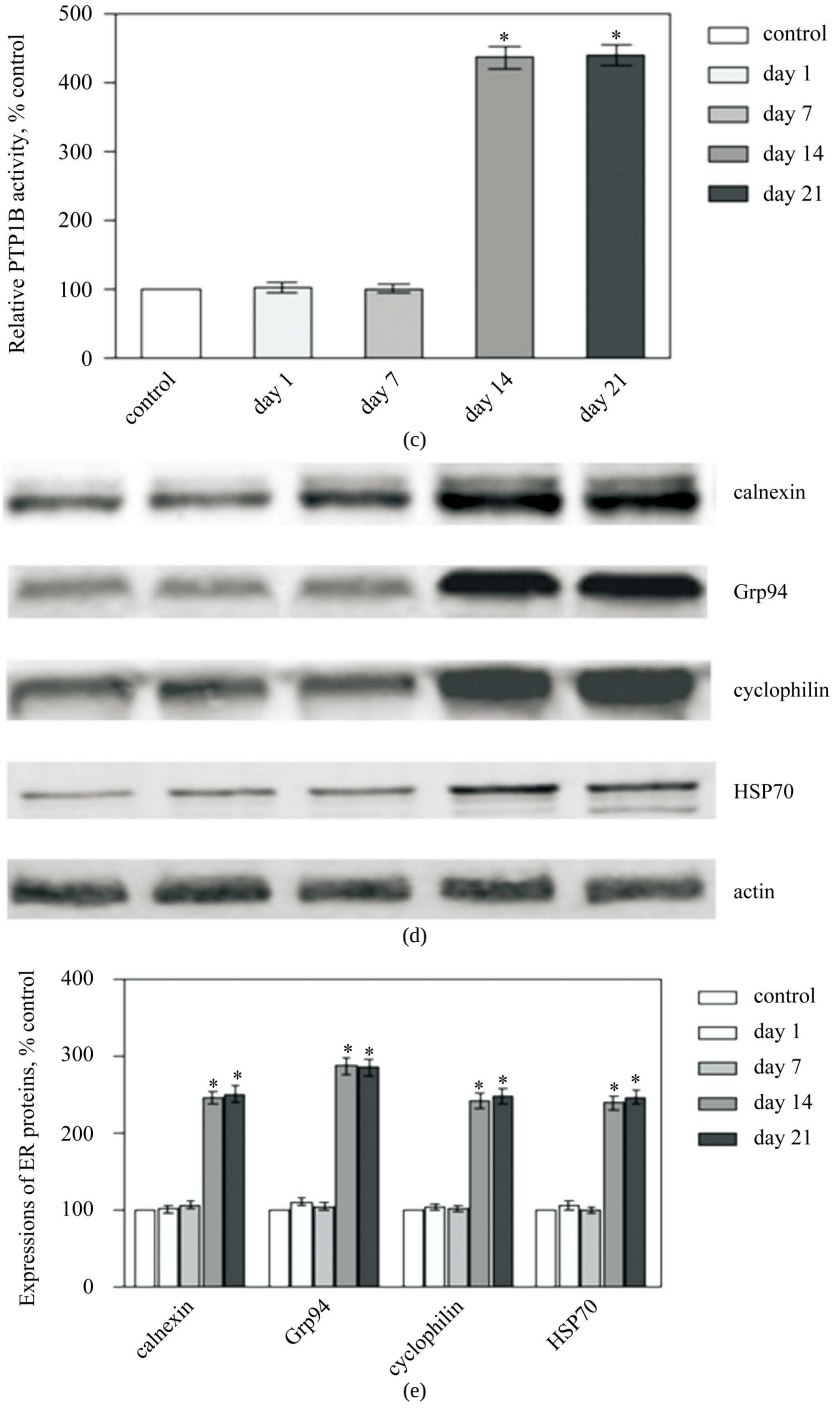

Figure 1. Timely alteration of ER in response to muscle mobilization. $Fyn^{+/-}$ and $Fyn^{-/-}$ mice were undergone leg casting, 1, 7, 14 and 21 days later (n = 5 for each group), gastrocnemius was collected and homogenized. (a) Change in $[Ca^{2+}]i$ was detected by fluorescence unit (RFU). $Fyn^{+/-}$ were undergone above operation, gastrocnemius was collected and homogenized; (b) ER and nuclear were separated, Fyn activity was detected by *in vitro* kinase assay; (c) PTP1B activity was detected by in vitro phosphatase assay; (d) and (e) Expressions of ER proteins including calnexin, Grp94, cyclophilin and Hsp70 were measured by Western Blot analysis. Data are normalized and calculated as the percentage of control, each value is the mean ± SEM for 5 independent experiments. $^{*}p < 0.05$ vs control.

activity remained at control level at day 1 - 7 following muscle mobilization, however, by day 14 - 21, which was considerably strengthened to 4.4 folds over control (**Figure 1(c)**). Furthermore, ER proteins (calnexin, Grp94, cyclophilin and HSP70) were measured by Western Blot analysis, it was demonstrated that whose expression was remarkably and timely increased by day 14 - 21, the levels were increased to 2.4 - 2.9 fold over control respectively (**Figure 1(d)**, **Figure 1(e)**).

3.2. Decrease in Membrane Protein Synthesis during Muscle Mobilization

It was previously reported that ER is associated with protein synthesis [26] [27], the functional alteration was proposed to implicate in the cellular responses during prolonged muscle denervation [8] [9]. In the present study, $Fyn^{(+/-)}$ mice were undergone leg casting, gastrocnemius was separated, **Figure 2(a)** revealed that protein synthesis in membrane was markedly decreased by day 14 following muscle mobilization, however, protein breakdown was increased in the same time (**Figure 2(b)**, **Figure 2(c)**).

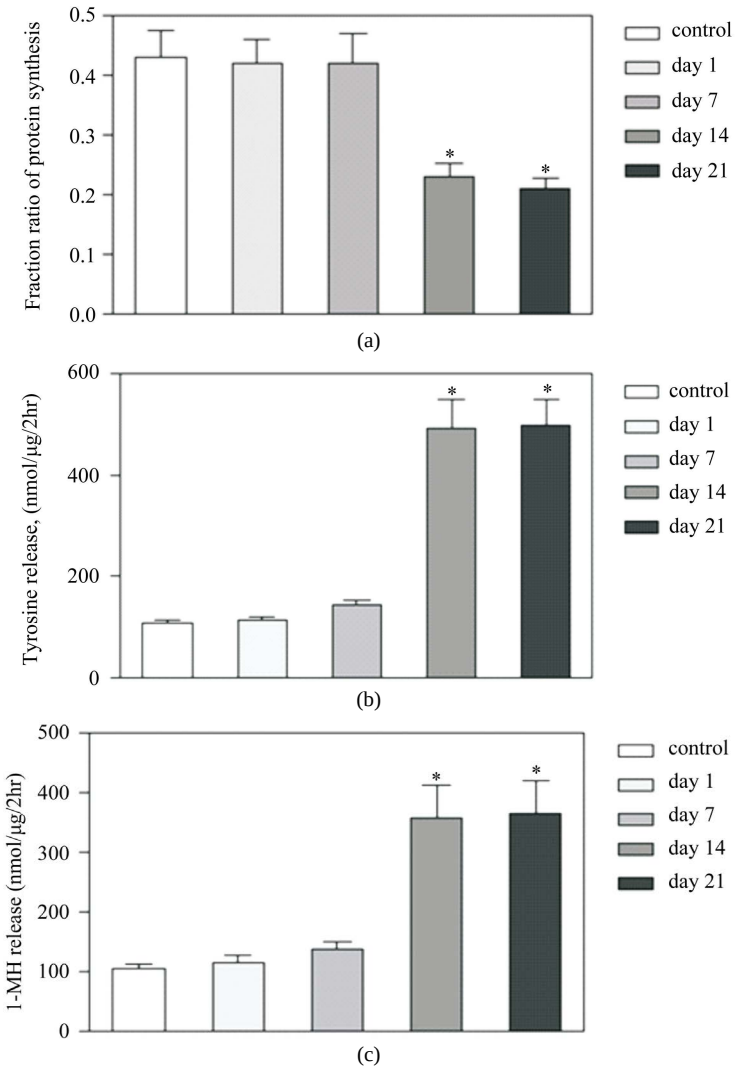

Figure 2. Decrease in membrane protein synthesis during muscle mobilization. $Fyn^{+/-}$ mice were undergone leg casting, 1, 7, 14 and 21 days later (n = 5 for each group), gastrocnemius was collected and homogenized. (a) Protein synthesis was detected by photocytometry; (b) and (c) Tyrosine and 1-MH release was detected using HPLC. Data are normalized and calculated as the percentage of control, each value is the mean ± SEM for 5 independent experiments. $^{*}p < 0.05$ vs control.

3.3. Membrane G$\beta1\gamma2$ Expression during Muscle Mobilization

Gastrocnemius was separated from Fyn$^{(+/-)}$ and Fyn$^{(-/-)}$ mice, by Western Blot analysis, signal quantification revealed that G$\beta1\gamma2$ membrane expression was greatly disrupted in Fyn$^{-/-}$ mice (**Figure 3(a)**). When Fyn$^{(+/-)}$ mice were undergone leg casting, it was revealed that G$\beta1\gamma2$ membrane expression in gastrocnemius was attenuated by day 14 following muscle mobilization (**Figure 3(b)**, **Figure 3(c)**). In parallel, PI3K-Akt signaling was considerably down-regulated (**Figure 3(d)**, **Figure 3(e)**).

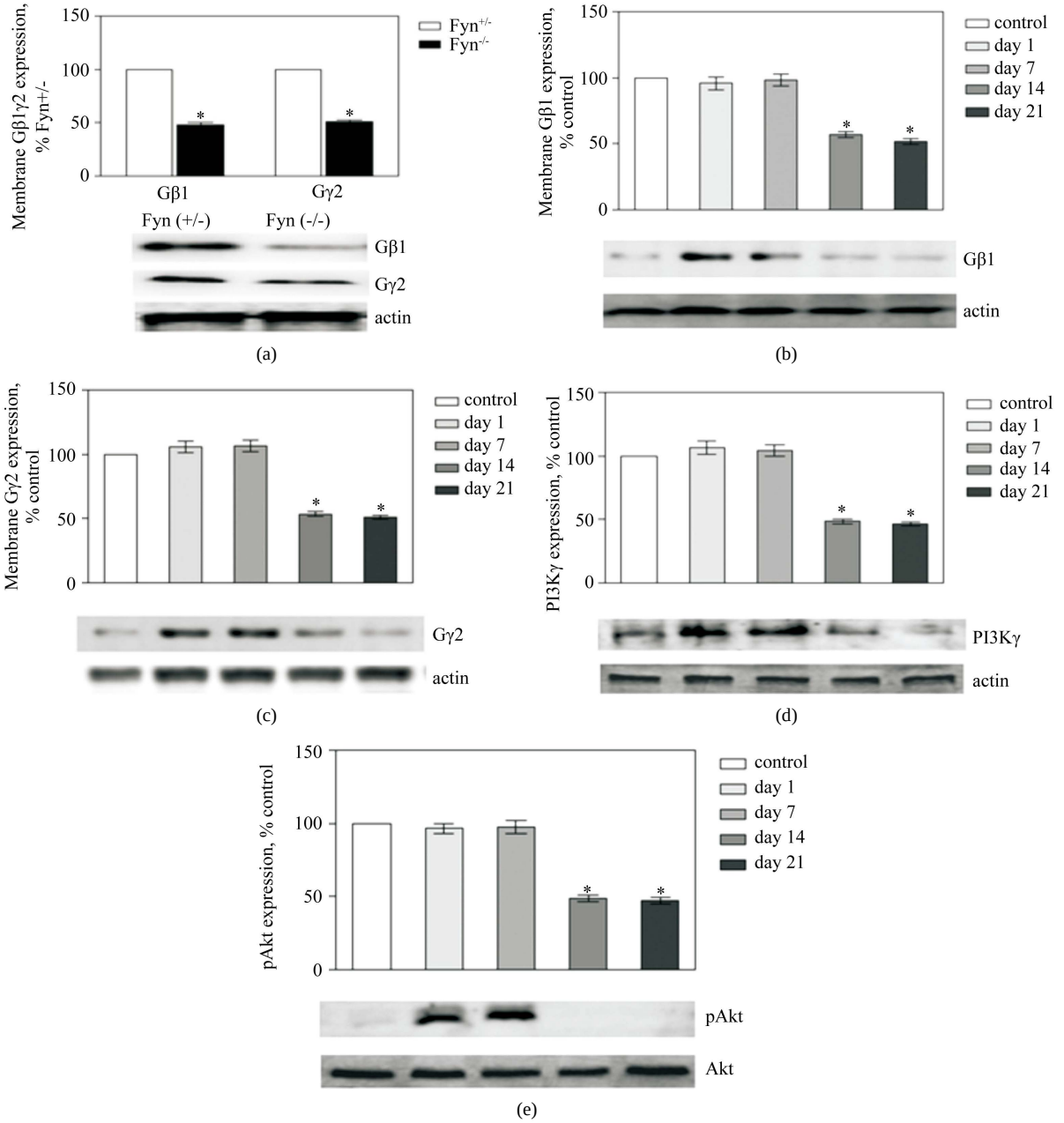

Figure 3. Membrane G$\beta1\gamma2$ expression during muscle mobilization. **(**a) Fyn$^{+/-}$ and Fyn$^{-/-}$ mice were used, gastrocnemius was collected and homogenized, membrane was separated, expressions of G$\beta1\gamma2$ were detected by Western Blot analysis. Fyn$^{+/-}$ mice were undergone leg casting, 1, 7, 14 and 21 days later (n = 5 for each group), gastrocnemius was collected and homogenized; (b) and (c) Membrane was separated, expressions of G$\beta1\gamma2$ were detected by Western Blot analysis; (d) and (e) Expressions of PI3Kγ and pAkt were detected by Western Blot analysis. Data are normalized and calculated as the percentage of control, each value is the mean ± SEM for 5 independent experiments. $^{*}p < 0.05$ vs *c*ontrol.

3.4. Membrane G$\beta 1\gamma 2$ Expression Was Dependent on ER Functional Alteration

Satellite cells were cultured to detect the modulation of G$\beta 1\gamma 2$ membrane expression, as illustrated in **Figure 4(a)**, G$\beta 1\gamma 2$ membrane expression was remarkably inhibited when exposed to brefeldin A (Golgi transport block, 10 μg/ml, 16 h), turnicamycin (N glycosylation block, 2 μg/ml, 18 h), or leptomycin B (nuclear export block, 20 nM, 30 min). PI3K-Akt signaling was attenuated in the same condition (**Figure 4(b)**, **Figure 4(c)**), then the data indicated that ER functional alteration might lead to G$\beta 1\gamma 2$ internalization and the resultant disruption of G-protein coupled receptor signaling.

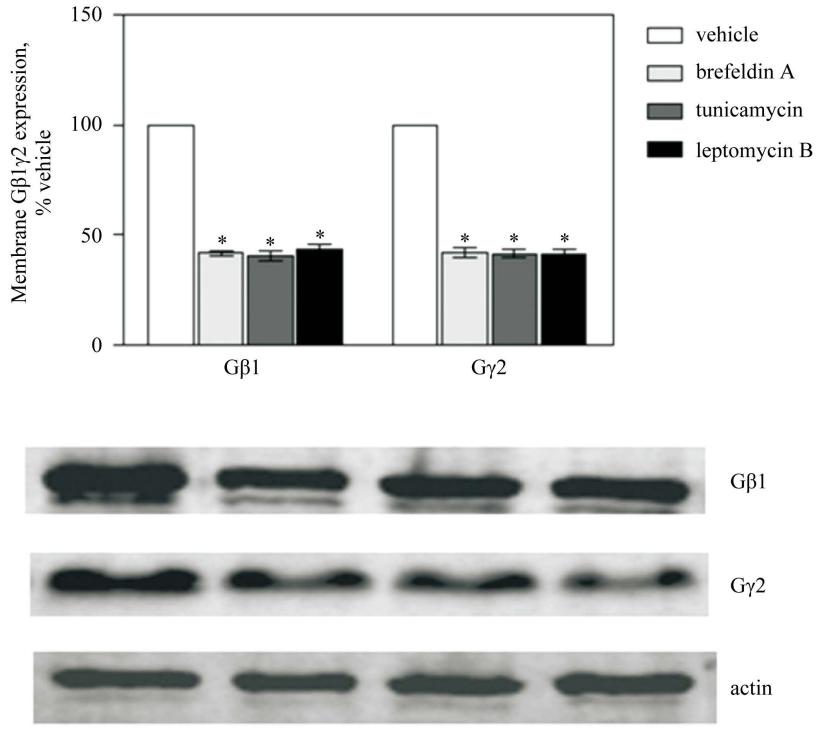

(a)

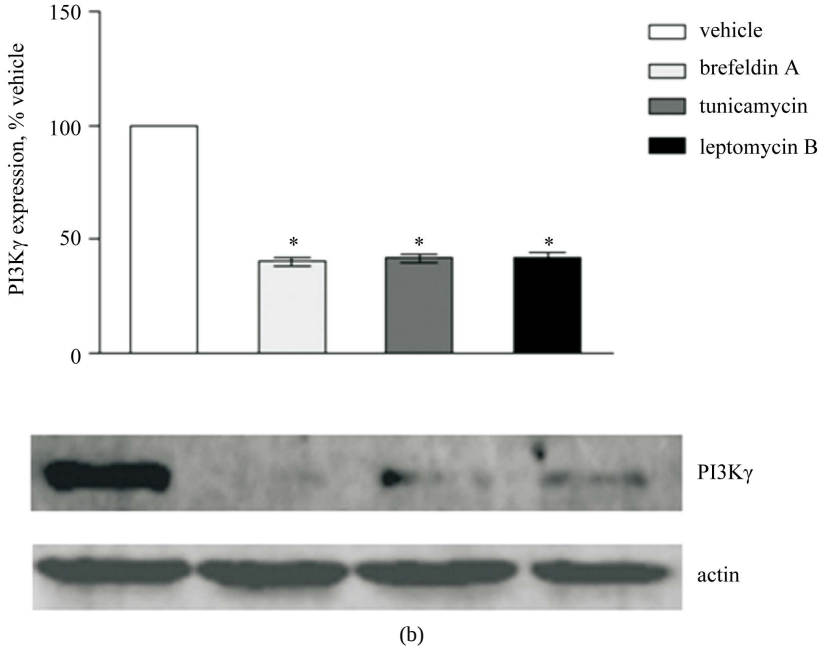

(b)

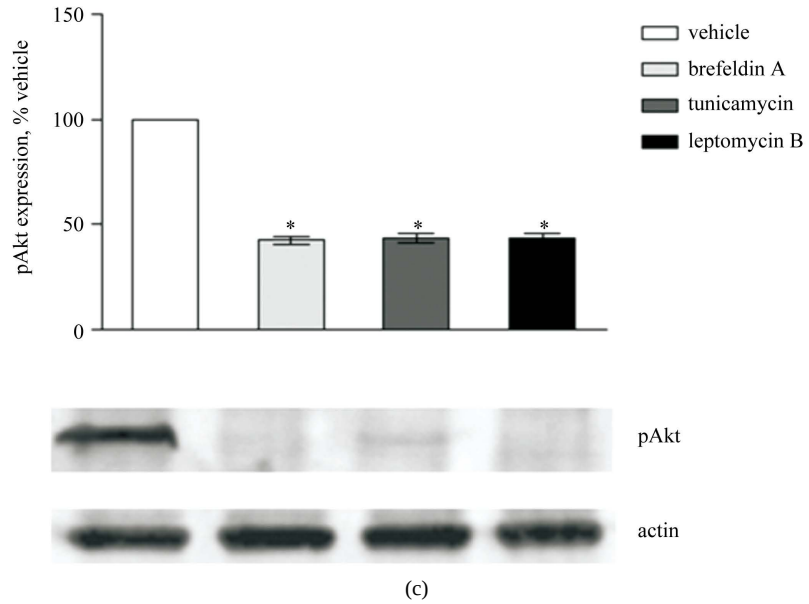

Figure 4. Membrane G$\beta1\gamma2$ expression was dependent on ER functional alteration. Satellite cells were cultured in the presence of brefeldin A, turnicamycin or lepromycin B for the indicated time. (a) Membrane was separated, expressions of G$\beta1\gamma2$ were detected by Western Blot analysis; (b) and (c) Expressions of PI3Kγ and pAkt were detected by Western Blot analysis. Data are normalized and calculated as the percentage of control, each value is the mean ± SEM for 5 independent experiments. $^{*}p < 0.05$ vs vehicle.

3.5. G$\beta1\gamma2$ Internalization Was Modulated by Rab1

By immunofluorescent analysis, it was illustrated that there was no detectable alteration in total G$\beta1\gamma2$ fluorescent densities, intriguingly, the fluorescence was considerably translocated into cytosol at day 14 following muscle mobilization (**Figure 5(a)**). Subsequently, molecular connection of Rab1 and G$\beta1\gamma2$ was detected by immunoprecipitation, in which anti-Rab1 was used as immunoprecipitated antibody and anti-G$\beta1\gamma2$ as immunoblot antibody, it was demonstrated that the expression levels were strengthened around 3.0 folds over control at 14 days following muscle mobilization (**Figure 5(b)**). Additionally, in satellite cells, by Western Blot analysis, it was revealed that there was a significant decrease in membrane G$\beta1\gamma2$ expression upon challenged with macrophage or T cell conditioned medium, the effect could be blocked by Rab1 knockdown (**Figure 5(c)**, **Figure 5(d)**). In the same time, satellite cell proliferation was disrupted in the presence of macrophage or T cell conditioned medium, the effect was dependent on Rab1 (**Figure 5(e)**).

3.6. G$\beta1\gamma2$ Internalization Was Associated with Motor Endplate Alteration

G$\beta1\gamma2$ and Rab1 were over- or down-expressed in gastrocnemius, then mice were undergone leg casting, it was revealed that cell survival was decreased considerably at day 14 - 21 following muscle mobilization: the levels reduced to 54.1 ± 6.1 and 53.1% ± 5.9% control respectively, which could be partly rescued in the presence of adeno-G$\beta1\gamma2$ or Rab1 siRNA (**Figure 6(a)**). Similarly, MuSK activity and AchR cluster, as well as muscle mechanical power was disrupted at day 14 following muscle mobilization, which could also be partly ameliorated by infection of adeno-G$\beta1\gamma2$ or Rab1 siRNA (**Figure 6(b)** and **Figure 6(c)**).

4. Discussion

Previously, we reported that timely Fyn activation triggered a particular microenvironment in the denervated gastrocnemius, which evoked early muscular inflammation and later local immunological changes via specific subcellular communication [8] [9]. Herein, gastrocnemius mobilization was established and it was observed that extracellular calcium level was elevated, which happened rapidly and sustained within one week of operation.

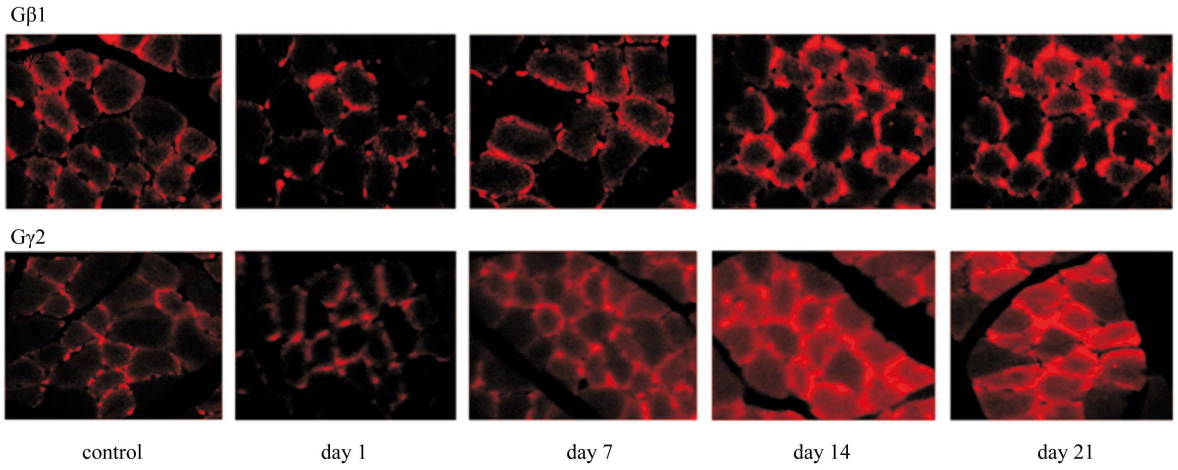
Gβ1
Gγ2
control
day 1
day 7
day 14
day 21

(a)

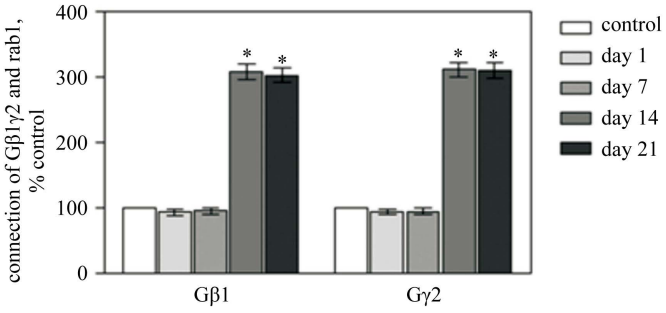
connection of Gβ1γ2 and rab1, % control
400
300
200
100
0
Gβ1
Gγ2
control
day 1
day 7
day 14
day 21


IP: rab 1
IB: Gβ1
IB: Gγ2

(b)

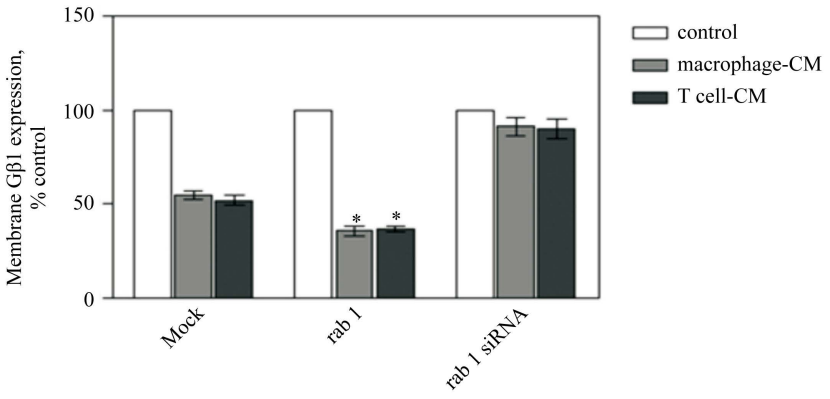
Membrane Gβ1 expression, % control
150
100
50
0
Mock
rab 1
rab 1 siRNA
control
macrophage-CM
T cell-CM


Mock
rab 1
rab 1 siRNA
Gβ1
actin

(c)

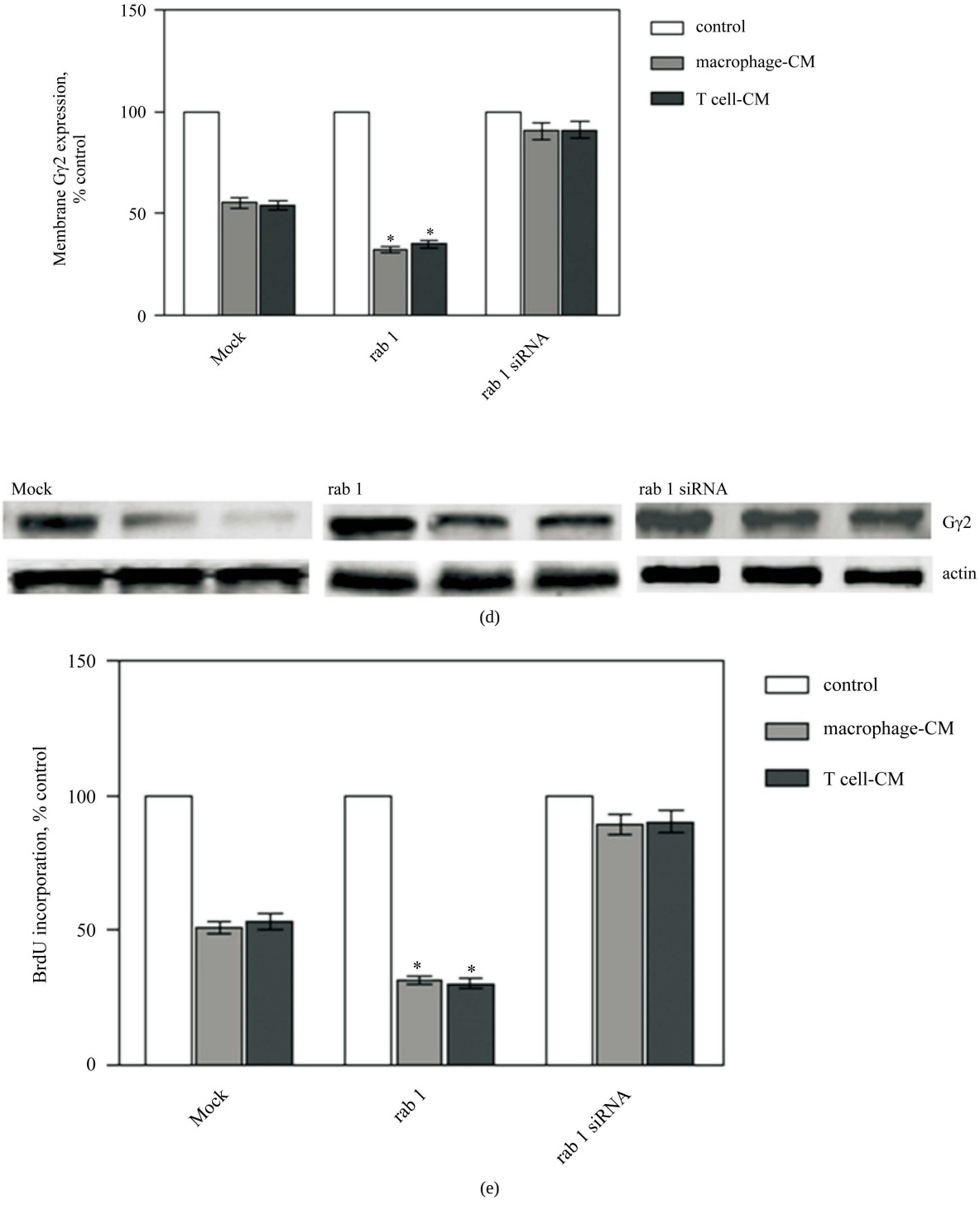

Figure 5. G$\beta 1\gamma 2$ internalization was modulated by Rab1. Fyn$^{+/-}$ mice were undergone leg casting, 1, 7, 14 and 21 days later (n = 5 for each group), gastrocnemius was collected. (a) Consecutive cryosections were immuno-stained with antibody against G$\beta 1\gamma 2$, Scale bar = 50 μm; (b) Connection of G$\beta 1\gamma 2$ and Rab1 was measured by immunoprecipitation, in which anti-Rab1 was used as immunoprecipitated antibody and anti-G$\beta 1\gamma 2$ as immuno-blot antibody. Satellite cells were cultured in the presence of adeno-Rab1 or adeno-Rab1 siRNA, then exposed to macrophage or T cell conditioned medium; (c) and (d) Expressions of G$\beta 1\gamma 2$ were determined by Western Blot analysis; (e) Cell survival was measured by BrdU incorporation. Data are normalized and calculated as the percentage of control, each value is the mean ± SEM for 5 independent experiments. $^{*}p < 0.05$ vs control.

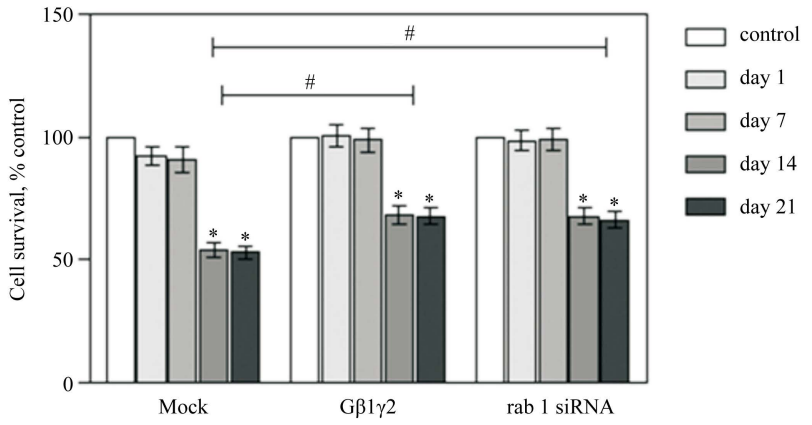
150
100
50
0
Cell survival, % control
#
#
*
*
*
*
*
*
Mock
Gβ1γ2
rab 1 siRNA
control
day 1
day 7
day 14
day 21

(a)

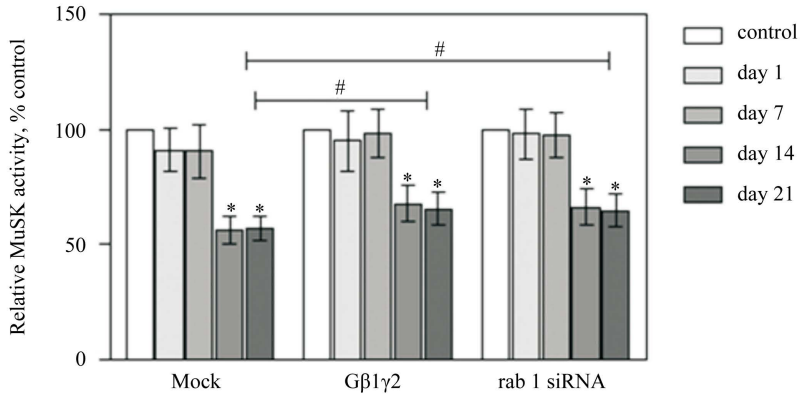
150
100
50
0
Relative MuSK activity, % control
#
#
*
*
*
*
*
*
Mock
Gβ1γ2
rab 1 siRNA
control
day 1
day 7
day 14
day 21

(b)

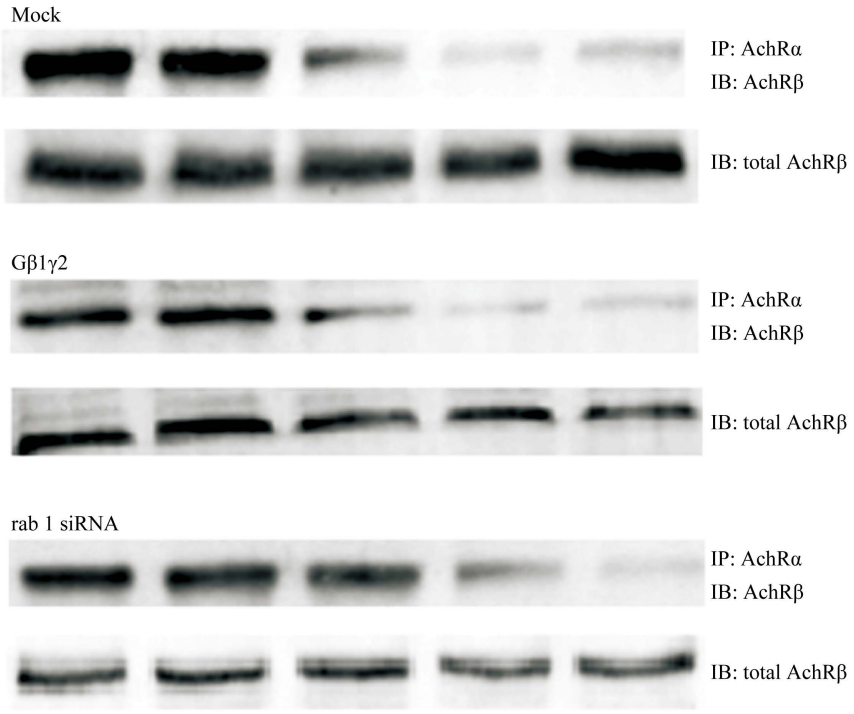
Mock
IP: AchRα
IB: AchRβ
IB: total AchRβ
Gβ1γ2
IP: AchRα
IB: AchRβ
IB: total AchRβ
rab 1 siRNA
IP: AchRα
IB: AchRβ
IB: total AchRβ

(c)

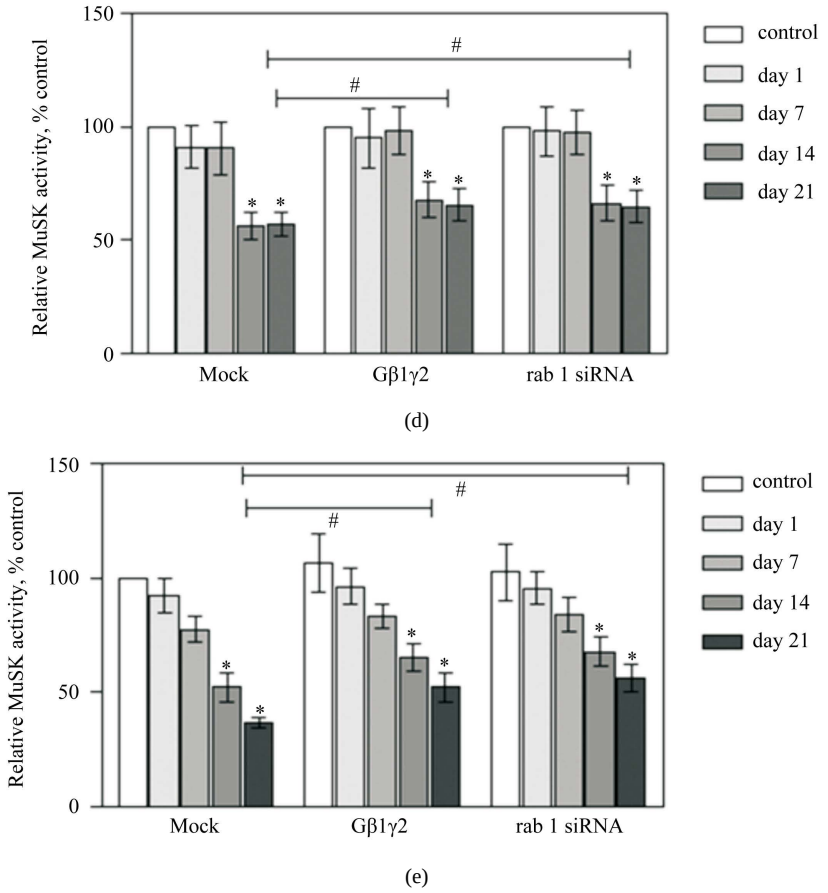

Figure 6. Gβ1γ2 internalization was associated with motor endplate alteration. Fyn$^{+/-}$ mice were locally injected with adeno-Gβ1γ2 or rab1 siRNA (5×10^9 pfu/day), then undergone leg casting, 1, 7, 14 and 21 days later (n = 5 for each group), gastrocnemius was collected and homogenized. (a) Cell survival was detected by MTT assay; (b) MuSK activity was determined by *in vitro* kinase assay; (c) and (d) AchR cluster was measured by immuno-precipitation, in which anti-AchRα was used as immunoprecipitated antibody and anti-AchRβ as immuno-blot antibody; (e) Muscle mechanical power was determined by vertical muscle apparatus. Data are normalized and calculated as the percentage of control, each value is the mean ± SEM for 5 independent experiments. $^*p < 0.05$ vs control.

Intriguingly, the elevation was sensitive to Fyn and could be partly inhibited by thapsigargin, a ER Ca^{2+} ATPase. Coincidently, we showed that Fyn activity was timely inhibited during muscle mobilization, which accompanied by enhanced PTP1B activity and expression of ER proteins (calnexin, Grp94, cyclophilin, and Hsp70). Thereby the present observations supported previous observation that muscle atrophy was related to PTP1B evoked organelle interconnection [10] [28]-[34], and provoked the idea that signaling in the ER compartment was proposed to feature and trigger certain distinctive functional outcomes during muscle mobilization.

Moreover, we demonstrated that prolonged muscle mobilization resulted in a remarkable increase in membrane protein breakdown and decrease in protein synthesis. In parallel, Gβ1γ2 appeared to be targeted and led to disruption in PI3K-Akt signaling. Recently, substantial evidence implicated that G-protein coupled receptors play an important role on skeletal muscle growth and differentiation, whose cross-talk with growth factor receptors make the host less vulnerable to the insults [35] [36]. Regarding current observation, Gβ1γ2 was presumed to be sensitized by muscle mobilization and might perpetuate and lower the threshold for musular dysfunction.

Coincidently, we observed that in later stage (14 - 21 day) of leg casting, Gβ1γ2 underwent vigorous internalization and cross-link with Rab1, a molecule for transport from ER to Golgi, this cellular event was primarily initiated in the presence of macrophage or T cells. Then, the data indicated that along with prolonged muscle

mobilization, Gβ1γ2 was translocated into ER, which seemed to result in marked impairment in the related G-protein couple receptor signaling. Additionally, it was illustrated that cross-link of Gβ1γ2 and Rab1 caused an increased decay of PI3K-Akt signaling and decrement of muscle cell survival. Therefore, a teleological argument is Gβ1γ2 translocation might trigger complex alterations in ER compartment, by which result in dynamic and variable damage to muscular function [37]-[41].

Skeletal muscle had the capacity to change its phenotype in response to altered functional demands, muscle atrophy was usually in parallel to the decline in protein synthesis and metabolism in motor endplate, and harbored different endogenous levels of muscle-specific tyrosine kinase (MuSK) and AchR cluster [42]-[46]. In the present study, we demonstrated that inhibition of Gβ1γ2-Rab1 cross-link appeared to be able to rescue muscular function, including reorganization of muscle cell viability, agrin initiated MuSK activity and AchR cluster, as well as muscle mechanical power. Therefore, we realized that stability of ER compartment was proposed to be important for the maintenance of muscular function, which could be deteriorated along with muscle mobilization.

5. Conclusion

Collectively, we demonstrated a dramatic and temporal up-regulation of extracellular calcium level during muscle mobilization, which was sensitive to Fyn and partly dependent on ER function. Coincidently, Fyn activity in ER was decreased with prolonged muscle mobilization, which was accompanied by enhanced PTP1B activity and expressions of ER proteins including calnexin, Grp94, cyclophilin, and Hsp70; in parallel, there was more protein breakdown than protein synthesis in membrane, which probably featured robust Gβ1γ2 internalization, and Rab1-related transport into ER compartment. Most importantly, muscle mobilization resulted in disruption of PI3K-Akt signaling and decrement of muscular functions, including muscle cell survival, agrin initiated MuSK activity as well as AchR cluster, and muscle mechanical power, which could be rescued by inhibition of Gβ1γ2-Rab1 cross-link. Thus, stability of ER compartment might overlap with stability of motor end-plate, which is a key component necessary for the early recovery processes regarding muscle atrophy, and would be the therapeutic considerations for muscle repair and regeneration.

Acknowledgements

This work is supported by the Natural scientific program in Minhang District of Shanghai (2011MHZ21), National nature sciences of China (81471370).

References

[1] Fitts, R.H., Romatowski, J.G., Blaser, C., De La Cruz, L., Gettelman, G.J. and Widrick, J.J. (2000) Effect of Spaceflight on the Isotonic Contractile Properties of Single Skeletal Muscle Fibers in the Rhesus Monkey. *Journal of Gravitational Physiology*, **7**, S53-S54.

[2] Marshall, J.M. and Tandon, H.C. (1984) Direct Observations of Muscle Arterioles and Venules Following Contraction of Skeletal Muscle Fibres in the Rat. *Journal of Physiology*, **350**, 447-459. http://dx.doi.org/10.1113/jphysiol.1984.sp015211

[3] Bruns, A.F., Bao, L., Walker, J.H. and Ponnambalam, S. (2009) EGF-A-Stimulated Signalling in Endothelial Cells via a Dual Receptor Tyrosine Kinase System Is Dependent on Co-Ordinated Trafficking and Proteolysis. *Biochemical Society Transactions*, **37**, 1193-1197. http://dx.doi.org/10.1113/jphysiol.1984.sp015211

[4] Prelle, K., Wobus, A.M., Krebs, O., Blum, W.F. and Wolf, E. (2000) Overexpression of Insulin-Like Growth Factor-II in Mouse Embryonic Stem Cells Promotes Myogenic Differentiation. *Biochemical and Biophysical Research Communications*, **277**, 631-638. http://dx.doi.org/10.1113/jphysiol.1984.sp015211

[5] Rosen, K.M., Wentworth, B.M., Rosenthal, N. and Villa-Komaroff, L. (1993) Specific, Temporally Regulated Expression of the Insulin-Like Growth Factor II Gene During Muscle Cell Differentiation. *Endocrinology*, **133**, 474-481. http://dx.doi.org/10.1210/en.133.2.474

[6] Hirashima, M., Ogawa, M., Nishikawa, S., Matsumura, K., Kawasaki, K., Shibuya, M. and Nishikawa, S. (2003) A Chemically Defined Culture of VEGFR2$^+$ Cells Derived from Embryonic Stem Cells Reveals the Role of VEGFR1 in Tuning the Threshold for VEGF in Developing Endothelial Cells. *Blood*, **101**, 2261-2267. http://dx.doi.org/10.1182/blood-2002-01-0003

[7] Nielsena, S. and Pedersena, B.K. (2008) Skeletal Muscle as an Immunogenic Organ. *Current Opinion in Pharmacology*, **8**, 346-351. http://dx.doi.org/10.1016/j.coph.2008.02.005

[8] Hanwei, H. and Zhao, H. (2010) FYN-Dependent Muscle-Immune Interaction after Sciatic Nerve Injury. *Muscle & Nerve*, **42**, 70-77. http://dx.doi.org/10.1002/mus.21605

[9] Zhao, H. and Huang, H. (2012) Functional Capability of IL-15-Akt Signaling in the Denervated Muscle. *Cytokine*, **60**, 608-615. http://dx.doi.org/10.1016/j.cyto.2012.08.026

[10] Zhao, H., Huang, H.W., Wu, J.G. and Huang, P.Y. (2013) Specialization of Mitochondrial and Vascular Oxidant Modulated VEGFR in the Denervated Skeletal Muscle. *Cell Signal*, **25**, 2106-2114. http://dx.doi.org/10.1016/j.cellsig.2013.06.014

[11] McGarrigle, D. and Huang, X.Y. (2007) GPCRs Signaling Directly through Src-Family Kinases. *Science Signaling*, **2007**, pe35. http://dx.doi.org/10.1126/stke.3922007pe35

[12] Zhao, H., Wu, G. and Cao, X. (2013) EGFR Dependent Subcellular Communication Was Responsible for Morphine Mediated AC Superactivation. *Cellular Signalling*, **25**, 417-428. http://dx.doi.org/10.1016/j.cellsig.2012.10.016

[13] Slessareva, J.E., Routt, S.M., Temple, B., Bankaitis, V.A. and Dohlman, H.G. (2006) Activation of the Phosphatidylinositol 3-Kinase Vps34 by a G Protein Alpha Subunit at the Endosome. *Cell*, **126**, 191-203. http://dx.doi.org/10.1016/j.cell.2006.04.045

[14] Hunyady, L., Baukal, A.J., Gaborik, Z., Olivares-Reyes, J.A., Bor, M., Szaszak, M., Lodge, R., Catt, K.J. and Balla, T. (2002) Differential PI 3-Kinase Dependence of Early and Late Phases of Recycling of the Internalized AT1 Angiotensin Receptor. *Journal of Cell Biology*, **157**, 1211-1222. http://dx.doi.org/10.1083/jcb.200111013

[15] Houle, S. and Marceau, F. (2003) Wortmannin Alters the Intracellular Trafficking of the Bradykinin B2 Receptor: Role of Phosphoinositide 3-Kinase and Rab5. *Biochemical Journal*, **375**, 151-158. http://dx.doi.org/10.1042/BJ20030872

[16] Kalia, M., Kumari, S., Chadda, R., Hill, M.M., Parton, R.G. and Mayor, S. (2006) Arf6-Independent GPI-Anchored Protein-Enriched Early Endosomal Compartments Fuse with Sorting Endosomes via a Rab5/phosphatidy-linositol-3'-kinase-Dependent Machinery. *Molecular Biology of the Cell*, **17**, 3689-3704. http://dx.doi.org/10.1091/mbc.E05-10-0980

[17] Riek, R.P., Handschumacher, M.D., Sung, S.S., Tan, M., Glynias, M.J., Schluchter, M.D., Novotny, J. and Graham, R.M. (1995) Evolutionary Conservation of both the Hydrophilic and Hydrophobic Nature of Transmembrane Residues. *Journal of Theoretical Biology*, **172**, 245-258. http://dx.doi.org/10.1006/jtbi.1995.0021

[18] Hynes, T.R., Tang, L., Mervine, S.M., Sabo, J.L., Yost, E.A., Devreotes, P.N. and Berlot, C.H. (2004) Visualization of G Protein $\beta\gamma$ Dimers Using Bimolecular Fluorescence Complementation Demonstrates Roles for Both β and γ in Subcellular Targeting. *Journal of Biological Chemistry*, **279**, 30279-30286. http://dx.doi.org/10.1074/jbc.M401432200

[19] Hynes, T.R., Mervine, S.M., Yost, E.A., Sabo, J.L. and Berlot, C.H. (2004) Live Cell Imaging of Gs and the β2-Adrenergic Receptor Demonstrates that Both Alphas and $\beta1\gamma7$ Internalize upon Stimulation and Exhibit Similar Trafficking Patterns That Differ from that of the β2-Adrenergic Receptor. *Journal of Biological Chemistry*, **279**, 44101-44112. http://dx.doi.org/10.1074/jbc.M405151200

[20] Saini, D.K., Kalyanaraman, V., Chisari, M. and Gautam, N. (2007) A Family of G Protein $\beta\gamma$ Subunits Translocate Reversibly from the Plasma Membrane to Endomembranes on Receptor Activation. *Journal of Biological Chemistry*, **282**, 24099-24108. http://dx.doi.org/10.1074/jbc.M701191200

[21] Jamora, C., Yamanouye, N., Van Lint, J., Laudenslager, J., Vandenheede, J.R., Faulkner, D.J. and Malhotra, V. (1999) G$\beta\gamma$-Mediated Regulation of Golgi Organization Is through the Direct Activation of Protein Kinase D. *Cell*, **98**, 59-68. http://dx.doi.org/10.1016/S0092-8674(00)80606-6

[22] Díaz Añel, A.M. and Malhotra, V. (2005) PKCη Is Required for $\beta1\gamma2/\beta3\gamma2$- and PKD-Mediated Transport to the Cell Surface and the Organization of the *Golgi apparatus*. *Journal of Cell Biology*, **169**, 83-91. http://dx.doi.org/10.1083/jcb.200412089

[23] Sönnichsen, B., De Renzis, S., Nielsen, E., Rietdorf, J. and Zerial, M. (2000) Distinct Membrane Domains on Endosomes in the Recycling Pathway Visualized by Multicolor Imaging of Rab4, Rab5, and Rab11. *Journal of Cell Biology*, **149**, 901-914. http://dx.doi.org/10.1083/jcb.149.4.901

[24] Zerial, M. and McBride, H. (2001) Rab Proteins as Membrane Organizers. *Nature Reviews Molecular Cell Biology*, **2**, 107-117. http://dx.doi.org/10.1038/35052055

[25] Miaczynska, M. and Zerial, M. (2002) Mosaic Organization of the Endocytic Pathway. *Experimental Cell Research*, **272**, 8-14. http://dx.doi.org/10.1006/excr.2001.5401

[26] Deldicque, L. (2013) Endoplasmic Reticulum Stress in Human Skeletal Muscle: Any Contribution to Sarcopenia? *Frontiers in Physiology*, **4**, 236. http://dx.doi.org/10.3389/fphys.2013.00236

[27] Veeranki, S. and Tyagi, S.C. (2013) Defective Homocysteine Metabolism: Potential Implications for Skeletal Muscle Malfunction. *International Journal of Molecular Sciences*, **14**, 15074-15091. http://dx.doi.org/10.3390/ijms140715074

[28] Anderie, I., Schulz, I. and Schmid, A. (2007) Direct Interaction between ER Membrane-Bound PTP1B and Its Plasma

Membrane-Anchored Targets. *Cellular Signalling*, **19**, 582-592. http://dx.doi.org/10.1016/j.cellsig.2006.08.007

[29] Frangioni, J.V., Beahm, P.H., Shifrin, V., Jost, C.A. and Neel, B.G. (1992) The Nontransmembrane Tyrosine Phosphatase PTP-1B Localizes to the Endoplasmic Reticulum via Its 35 Amino Acid C-Terminal Sequence. *Cell*, **68**, 545-560. http://dx.doi.org/10.1016/0092-8674(92)90190-N

[30] Frangioni, J.V., Oda, A., Smith, M., Salzman, E.W. and Neel, B.G. (1993) Calpain-Catalyzed Cleavage and Subcellular Relocation of Protein Phosphotyrosine Phosphatase 1B (PTP-1B) in Human Platelets. *EMBO Journal*, **12**, 4843-4856.

[31] Haj, F.G., Verveer, P.J., Squire, A., Neel, B.G. and Bastiaens, P.I. (2002) Imaging Sites of Receptor Dephosphorylation by PTP1B on the Surface of the Endoplasmic Reticulum. *Science*, **295**, 1708-1711. http://dx.doi.org/10.1126/science.1067566

[32] Hernandez, M.V., Sala, M.G., Balsamo, J., Lilien, J. and Arregui, C.O. (2006) ER-Bound PTP1B Is Targeted to Newly Forming Cell-Matrix Adhesions. *Journal of Cell Science*, **119**, 1233-1243. http://dx.doi.org/10.1242/jcs.02846

[33] Lorenzen, J.A., Dadabay, C.Y. and Fischer, E.H. (1995) COOH-Terminal Sequence Motifs Target the T Cell Protein Tyrosine Phosphatase to the ER and Nucleus. *Journal of Cell Biology*, **131**, 631-643. http://dx.doi.org/10.1083/jcb.131.3.631

[34] Li, S., Depetris, R.S., Barford, D., Chernoff, J. and Hubbard, S.R. (2005) Crystal Structure of a Complex between Protein Tyrosine Phosphatase 1B and the Insulin Receptor Tyrosine Kinase. *Structure*, **13**, 1643-1651. http://dx.doi.org/10.1016/j.str.2005.07.019

[35] Tonks, N.K. (2003) PTP1B: From the Sidelines to the Front Lines! *FEBS Letters*, **546**, 140-148. http://dx.doi.org/10.1016/S0014-5793(03)00603-3

[36] Gambardella, L. and Vermeren, S. (2013) Molecular Players in Neutrophil Chemotaxis—Focus on PI3K and Small GTPases. *Journal of Leukocyte Biology*, **94**, 603-612. http://dx.doi.org/10.1189/jlb.1112564

[37] Hanna, S. and El-Sibai, M. (2013) Signaling Networks of Rho GTPases in Cell Motility. *Cellular Signalling*, **25**, 1955-1961. http://dx.doi.org/10.1016/j.cellsig.2013.04.009

[38] Chua, C.E. and Tang, B.L. (2013) Linking Membrane Dynamics and Trafficking to Autophagy and the Unfolded Protein Response. *Journal of Cellular Physiology*, **228**, 1638-1640. http://dx.doi.org/10.1002/jcp.24341

[39] Liu, S. and Storrie, B. (2012) Are Rab Proteins the Link between Golgi Organization and Membrane Trafficking? *Cellular and Molecular Life Sciences*, **69**, 4093-4106. http://dx.doi.org/10.1007/s00018-012-1021-6

[40] Martinez, O. and Goud, B. (1998) Rab Proteins. *Biochimica et Biophysica Acta*, **1404**, 101-112. http://dx.doi.org/10.1016/S0167-4889(98)00050-0

[41] Goud, B. and McCaffrey, M. (1991) Small GTP-Binding Proteins and Their Role in Transport. *Current Opinion in Cell Biology*, **3**, 626-633. http://dx.doi.org/10.1016/0955-0674(91)90033-U

[42] Punga, A.R., Maj, M., Lin, S., Meinen, S. and Ruegg, M.A. (2011) MuSK Levels Differ between Adult Skeletal Muscles and Influence Postsynaptic Plasticity. *European Journal of Neuroscience*, **33**, 890-898. http://dx.doi.org/10.1111/j.1460-9568.2010.07569.x

[43] Rivas-Plata, K.A., Kraas, J.R., Saleh, S.M. and Swope, S.L. (2001) Src-Class Kinases Act within the Agrin/MuSK Pathway to Regulate Acetylcholine Receptor Phosphorylation, Cytoskeletal Anchoring, and Clustering. *Journal of Neuroscience*, **21**, 3806-3818.

[44] Smith, C.L., Mittaud, P., Prescott, E.D., Fuhrer, C. and Burden, S.J. (2001) Src, Fyn, and Yes Are Not Required for Neuromuscular Synapse Formation but Are Necessary for Stabilization of Agrin-Induced Clusters of Acetylcholine Receptors. *Journal of Neuroscience*, **21**, 3151-3160.

[45] Wang, Q., Zhang, B., Wang, Y.E., Xiong, W.C. and Mei, L. (2008) The Ig1/2 Domain of MuSK Binds to Muscle Surface and Is Involved in Acetylcholine Receptor Clustering. *Neurosignals*, **16**, 246-253. http://dx.doi.org/10.1159/000111567

[46] Willmann, R., Pun, S., Stallmach, L., Sadasivam, G., Santos, A.F., Caroni, P. and Fuhrer, C. (2006) Cholesterol and Lipid Microdomains Stabilize the Postsynapse at the Neuromuscular Junction. *EMBO Journal*, **25**, 4050-4060. http://dx.doi.org/10.1038/sj.emboj.7601288